Journal of Environmental Management 273 (2020) 111150

Contents lists available at ScienceDirect

Journal of Environmental Management

journal homepage: www.elsevier.com/locate/jenvman

Research article

Active biomass estimation based on ASM1 and on-line OUR measurements for partial nitrification processes in sequencing batch reactors

Franklin Lindow [a], Carlos Muñoz [b], Francisco Jaramillo [c], Robert H. Bishop [d], José B. Proal-Nájera [e], Christian Antileo [f,*]

[a] Ingenieurgesellschaft Prof. Dr. Sieker mbH, Rennbahnallee 109A, 15366 Hoppegarten, Germany
[b] Department of Electrical Engineering, University of La Frontera, Cas. 54-D, Temuco, Chile
[c] Department of Electrical Engineering, University of Chile, Av. Tupper 2007, Santiago, Chile
[d] Electrical Engineering, University of South Florida, 4202 E. Fowler Ave., Tampa, FL 33620, United States of America
[e] Instituto Politécnico Nacional. CIIDIR-Unidad Durango. Calle Sigma 119. Fracc. 20 de Noviembre II, Durango, Dgo., C.P. 34220, Mexico
[f] Department of Chemical Engineering, University of La Frontera, Cas. 54-D, Temuco, Chile

ARTICLE INFO

Keywords:
OUR
ASM1
State observer
Partial nitrification
Active biomass estimator

ABSTRACT

The main challenge for partial nitrification is to reach stable nitrite accumulation, which strongly depends on the nitrite-oxidizing bacteria (NOB) growth in the reactor. The on-line estimation of active biomass may enhance the decision-making process to maintain a high nitrite accumulation in the reactor. In this work, we propose an active biomass estimator based on ASM1 and on-line oxygen uptake rate measurements (OUR-E) in a sequencing batch reactor. In order to validate the OUR-E, two operating scenarios were applied during 200 days of operation: unfavorable (sludge retention time (SRT) = 40 d, pH = 7.6, dissolved oxygen (DO) = 2 mg/L) and favorable for partial nitrification (SRT = 10 d, pH = 8.5, DO = 2 mg/L). Furthermore, a second estimation method based on off-line measurements of N-species concentrations (Nsp-E) was implemented to evaluate the performance of the OUR-E. The OUR-E was able to predict a reduction in the NOB active fraction from 10.3% to 1.6% with nitrite accumulation over 80% when we shifted the operating scenario. Although both estimators predicted similar results, the OUR-E showed a better prediction quality than the Nsp-E, according to Theil's coefficient of inequality.

1. Introduction

Partial nitrification consists of incomplete biological oxidation of ammonia up to nitrite. For this purpose the environmental conditions are adjusted to inhibit nitrite-oxidizing bacteria (NOB) growth; ammonium is oxidized by ammonia-oxidizing bacteria (AOB) to nitrite (nitritation) and only a part of this nitrite is oxidized by NOB to nitrate (nitratation). The accumulated nitrite can be reduced in the denitrification step by heterotrophic bacteria (HB) and subsequently in various steps to molecular nitrogen. The application of partial nitrification has various advantages, such as the reduction of aeration costs (up to 25%), the amount of carbon needed in denitrification (up to 60%), and active sludge production (Pambrun et al., 2008; Peng and Zhu, 2006; Pollice et al., 2002). Partial nitrification depends on dissolved oxygen (DO) concentration, pH, ammonia concentration, temperature and the solids retention time (SRT) (Jaramillo et al., 2018b). Past research has shown how to obtain a stable shortcut nitrification process by combining some or all of these parameters; however, successful long-term partial nitrification (months to years) at industrial scale requires on-line monitoring of the microorganisms' activity in order to avoid a step-wise increase of nitrate concentration with the growth of NOB in the reactor. The latter can be explained by the acclimation of nitrifying biomass to the inhibiting or limiting conditions (Casellas et al., 2006; Turk and Mavinic, 1989). The required monitoring can be done on-line by measurement of the DO concentration (Ganesh et al., 2006; Garcia-Ochoa et al., 2010) based on correlating the bacterial growth rate with the oxygen uptake rate (OUR). This tool provides the possibility of detecting inhibitions (Hockenbury and Grady, 1977; Jubany et al., 2009) and can also be applied for control purposes, i.e. for maintaining a constant oxygen consumption rate inside the reactor (Jubany et al., 2009) or for detecting the endpoint of ammonia oxidation during a cycle in a sequencing batch reactor (SBR) (Chen et al., 2012; Corominas et al., 2011).

* Corresponding author.
E-mail addresses: f.lindow@sieker.de (F. Lindow), carlos.munoz@ufrontera.cl (C. Muñoz), francisco.jaramillo@ing.uchile.cl (F. Jaramillo), robertbishop@usf.edu (R.H. Bishop), joseproal@hotmail.com (J.B. Proal-Nájera), christian.antileo@ufrontera.cl (C. Antileo).

https://doi.org/10.1016/j.jenvman.2020.111150
Received 25 April 2020; Received in revised form 14 July 2020; Accepted 27 July 2020
Available online 5 August 2020
0301-4797/© 2020 Elsevier Ltd. All rights reserved.

Nomenclature

AOB	Ammonia-oxidizing bacteria
ASM1	Activated sludge model No. 1
DO*	Dissolved oxygen set-point
FISH	Fluorescent in-situ Hybridization
HB	Heterotrophic bacteria
K_{La}	Volumetric oxygen transport coefficient
NOB	Nitrite-oxidizing bacteria
Nsp-E	N-species estimation
OUR	Oxygen uptake rate [mg O_2/(L·h)]
OUR-E	Oxygen uptake rate estimation
pH*	pH set-point
r_s	Ammonia conversion rate [kg TAN/(kg SSV·d)]
SBR	Sequencing batch reactor
$S_{NO_2^-}$	Total nitrite nitrogen concentration (HNO_2–N + NO_2–N)
$S_{NO_3^-}$	Total nitrate nitrogen concentration (HNO_3–N + NO_3^-–N)
SQP	Sequential quadratic programming
SRT	Sludge retention time
S_{TAN}	Total ammonia nitrogen concentration (NH_3–N + NH_4^+–N)
TIC	Theil's inequality coefficient
X_0	Initial biomass concentration inside the reactor
X_A	Concentration of active AOB [mg COD/L]
X_{COD}	Particulate COD concentration [mg COD/L]
X_H	Concentration of active HB [mg COD/L]
X_N	Concentration of active NOB [mg COD/L]
X_{VSS}	Volatile suspended solid concentration [mg/L]
Y_A	Yield coefficient of AOB over substrate [g COD/g N]
Y_H	Yield coefficient of HB over substrate [g COD/g COD]
Y_N	Yield coefficient of NOB over substrate [g COD/g N]
$Y_{O_2/S}$	Yield coefficient of oxygen over substrate [g O_2/g COD] or [g O_2/g N]
$\%X_A$	Estimated fraction of active AOB ($\%X_A = X_A/X_{COD}$)
$\%X_N$	Estimated fraction of active NOB ($\%X_N = X_N/X_{COD}$)
$\%X_A+\%X_N$	Estimated fraction of active autotrophic bacteria
$\%X_{NA}$	Estimated fraction of active NOB among active autotrophic bacteria ($\%X_{NA} = X_N/(X_A+X_N)$)
α	Total TAN conversion (1-TAN_{end}/TAN) (%)
β	Total nitrite accumulation ($\Delta NO_2^-/(\Delta NO_2^- + \Delta NO_3^-)$) (%)

SBR is a compact technology with a small footprint, which offers several advantages: only one unit is required as reactor and settler; nitrification and denitrification may be conducted in the same reactor; flexibility in the loading rate; and real-time control strategies can be implemented allowing exact adjustment of the length of reaction phases to optimize energy consumption (Corominas et al., 2011; Jaramillo et al., 2018a). Additionally, SBR is very suitable for partial nitrification since it can detect when nitrite concentration reaches the maximum, avoiding subsequent oxidation to nitrate (Antileo et al., 2013; Jaramillo et al., 2018b).

A key factor for achieving long-term partial nitrification in SBRs is knowledge of the concentration of the active AOB, NOB, and HB in the reactor on a long-term basis. These active bacteria concentrations as unmeasured variables have a direct influence on the nitritation rate and therefore on the degree of nitrite accumulation for partial nitrification. Unfortunately, hardware sensors are not able to measure active biomass on-line; however, this can be overcome by using state estimators (also called soft-sensors). As shown in Fig. 1, state estimators calculate missing information about the internal states of a biochemical process (unmeasured variables), e.g. they can infer meaningful hidden information from the data provided by the sensor based on a model (Sotomayor et al., 2002). This method could be based on a phenomenological model, such as the ASM1 or data-driven models obtained from artificial intelligence techniques, or a combination of both.

Most known implementations of state estimators related to biological nitrogen removal are based on continuous processes (Alcaraz-González et al., 2002; Benazzi et al., 2007; Boulkroune et al., 2009; Hedegärd and Wik, 2011). The challenge in this work was to apply a state estimator for a transient state process, such as SBR, based on a modified ASM1; and to develop a new estimation method of internal variables using real-time differentiation of active AOB/NOB nitrifying biomass.

Bogaerts and Wouwer (2003) and Hedegärd and Wik (2011) have reported an implementation of estimators for continuous nitrogen removal processes in a simulated ASM1. Later, Smida et al. (2018a,b) reported an observer based on a continuous process and calibrated ASM1 with experimental data in order to develop a predictive control scheme. Wu et al. (2014) also used a predictive control approach to control the substrates in a continuous activated sludge. For online estimation of active biomass in SBR for partial nitrification, Boaventura et al. (2001) estimated the total active autotrophic and heterotrophic biomass concentrations. To our knowledge there is no work reporting the differentiated AOB and NOB estimation from OUR in real time.

Therefore, the objectives of this work were:

- To develop two new estimation methods of internal states of the partial nitrification process derived from the full-horizon state estimation, using a modified ASM1 model. The first estimator uses on-line oxygen uptake rate measurements (OUR-E) and the second one uses off-line measurements of N-species concentrations (Nsp-E).
- To estimate on-line the most likely initial conditions for the active bacteria concentrations in SBR cycles.
- To validate the two proposed estimators through experimental assays at two operating scenarios of an SBR on long-term basis.
- To compare the performance of the on-line estimator OUR-E with respect to the off-line estimator Nsp-E.

We developed a method for indirect and differentiated determination of the active concentrations of AOB, NOB and HB using state estimation based on on-line measurements of OUR and the initial concentrations of the N-species (NH_4^+, NO_2^-, NO_3^-) measured off-line. This state estimator is able to calculate the development of the concentrations of the N-species, OUR and the active concentrations of both bacterial species during an SBR-cycle by running multiple simulations of a modified ASM1 (ASM1 for partial nitrification). Most studies on SBR modeling are validated only in short time dynamics considering the behavior during a small number of cycles. In this work, the two proposed estimators were validated on a long-term basis by comparison of estimates with off-line measurements in order to determine the trend of the active NOB concentration during partial nitrification.

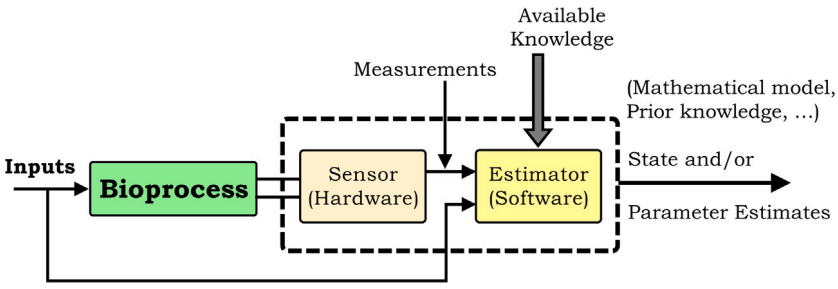

Fig. 1. Principle of a soft-sensor.
Source: Adapted from Sotomayor et al. (2002).

2. Materials and methods

2.1. Sequencing batch reactor

The lab-scale SBR had a volume of 2.4 L. Temperature was kept in a range around 20° C by a thermostat (JULABO, Model EC, Germany). Homogenization was performed by a stirrer at 360 rpm (HEIDOLPH, RSR 2050, Germany). DO and pH/temperature were measured by two electrodes, WTW (OXI 701, Germany) and HACH (EC 310, USA). The SBR system was automated with a programmable logic controller (PLC) (Siemens, Simatic S7-200, CPU214, Germany) and operated with a user interface developed in MATLAB® 7.1, linked to the PLC through the OPC (OLE for Process Control) server KepServerEX. The pH was regulated by a PI controller by the addition of 0.125 mL at 0.2M sodium carbonate solution with a diaphragm pump (LANG, model ELADOS, EMP II, 41 L/h, Germany) to neutralize the protons released during nitrification. DO control was carried out by applying pulse width modulation (PWM), with a time period of 1 s, to open an electromagnetic air valve (Festo, 457, MSG- 24DC, Germany). The aeration was supplied by a blower (COSMOS double type 1000, China). The synthetic solution used to feed the SBR was prepared in tap water as follows: $(NH_4)_2SO_4$, 4.52 g/L; $MgSO_4$ $7H_2O$, 0.256 g/L; K_2HPO_4, 1.7448 g/L; KH_2PO_4, 1.364 g/L.

The concentration of the N-species (e.g. ammonium, nitrite, nitrate) in a SBR cycle was determined once to twice a week, taking samples every fifty minutes during a cycle. The total ammonia nitrogen (TAN) concentration was measured by electrometry with a dual channel pH/ion meter (AR25 Fisher Scientific). The concentrations of nitrite and nitrate were measured using standard spectrophotometric methods (APHA, 1992) and UVmini-1240 UV–VIS-Spectrophotometers Shimadzu equipment.

The SBR was inoculated with sludge from the wastewater treatment plant of Temuco, Chile. The SRT was measured weekly in order to maintain the bacterial activity stable during the validation of the estimation methods, considering sample volumes for off-line measurements and the waste activated sludge. The biomass concentrations were determined by filtration, drying (105° C) and incineration (550° C).

The OUR was determined by the dynamic method, with aeration interrupted every 15 min for 33 s. It was determined experimentally that an interruption time shorter than 33 s led to unreliable OUR measurements. The DO concentration inside the reactor was determined every two seconds. For the OUR calculation only the DO values of the last fifteen seconds of the interruption were used, excluding the last measurement point and avoiding DO depletion below 1.5 mg O2/L according to Jubany et al. (2008, 2009). The $-dDO/dt$ slope of the linear regression of the curve DO vs time with the highest R^2 was used to calculate the OUR.

2.2. Control and operating strategies of the SBR

Partial nitrification was carried out in a SBR using four phases: filling, aerobic reaction, settling, and discharge. Uncompleted ammonia oxidation occurred up to nitrite (partial nitrification), and the progress of the reaction was evaluated on-line by detecting bending points as a real-time control strategy according to Antileo et al. (2013). This strategy detected the end point of ammonia oxidation when the diaphragm pump did not make a stroke for 30 min and a minimum value of %AVO (air valve opening) was reached. Afterwards, aeration was stopped, the sludge was allowed to settle inside the SBR for 30 min and the effluent was removed.

The SBR reactor was controlled in real-time by a PLC. One level higher in the hierarchic command order were two MATLAB® interfaces, one for the DO concentration control (DO-control) and the other for control of the SBR. The SBR control involved on-line processing and storage of pH/temperature, DO concentration and OUR. These acquired data enabled the PLC to command the stirrer, the sodium carbonate pump (actuator of pH control), air valve opening (actuator of DO control), and the charge and discharge pumps for the control of SBR cycles.

The estimation methods proposed in this work aimed to calculate the trends of the active biomass concentrations X_A (AOB), X_N (NOB) and X_H (HB) on a long-term basis. Therefore, two operating scenarios were carried out as shown in Table 1, one scenario favorable for partial nitrification and the other unfavorable. The favorable scenario involved a strongly alkaline pH since ammonia nitrogen inhibits NOB growth, and low SRT acts as kinetic selection pressure for NOB washout. In contrast, high SRT and a slightly alkaline environment promote AOB and NOB growth, leading to complete nitrification from ammonia up to nitrate. The DO concentration was high enough to enable OUR measurements on-line during each SBR cycle with a set-point of 2 mg/L by means of a predictive control based on a modified ASM1 model (Muñoz et al., 2009).

2.3. Modified ASM1 model

A modified model based on the ASM1 (Henze et al., 1987) was used to estimate the active biomass of autotrophic and heterotrophic microorganisms on-line during whole SBR cycles as well as to perform DO predictive control.

In ASM1, nitrification is represented as a one-step process with no differentiation between nitritation and nitratation (Gernaey et al., 2004). In this work, we added kinetic equations and yields of AOB and NOB species in the model matrix to simulate nitritation and nitratation. The modified ASM1, described in Eq. (1), uses eleven differential equations as state variables, considering kinetic parameters as well as growth, decay and hydrolysis parameters of both nitrifying species and state variables for the different fractions of soluble and particular matter. In addition, the first three state variables (S_{TAN}, $S_{NO_2^-}$, and $S_{NO_3^-}$) were considered as the output ($\boldsymbol{y_N}$) of this state–space system. The

Table 1
Operating conditions for the validation of the estimation methods.

	pH set-point	SRT [d]	DO set-point [mg O_2/L]	Time [d]
Unfavorable scenario for partial nitrification	7.6	~ 40	2.0	120
Favorable scenario for partial nitrification	8.5	~ 10	2.0	60

model matrix was based on the processes $\boldsymbol{\rho}(x)$, the rate equations, and the stoichiometry of the eleven compounds ($\boldsymbol{A}$), which are illustrated in Table 2. All the stoichiometric and kinetic parameters considered in the proposed model are detailed in Table 3. The kinetic equations for AOB and NOB originally involved substrate inhibitions ($[S_{NH3}]^2/K_{IS,A}$ and $[S_{HNO2}]^2/K_{IS,N}$) as well as cross inhibitory kinetics ($S_{NH3}/K_{I,N}$ and $C_{HNO2}/K_{I,A}$). Finally, the equations related to the two-step nitrification process are shown in Table 4.

$$\begin{aligned} \dot{\boldsymbol{x}}(t) &= \boldsymbol{A}^T \boldsymbol{\rho}(\boldsymbol{x}(t)) \\ \boldsymbol{y_N} &= \begin{bmatrix} x_1(t) & x_2(t) & x_3(t) \end{bmatrix}^T \\ \boldsymbol{x_0} &= \boldsymbol{x}(0) \\ \boldsymbol{x}(t) &= \begin{bmatrix} S_{TAN} & S_{NO_2^-} & S_{NO_3^-} & S_{ND} & S_S & X_A & X_N & X_H & X_P & X_S & X_{ND} \end{bmatrix}^T \end{aligned} \quad (1)$$

As an alternative output, Eq. (2) was used to predict the simultaneous respiration of the nitrifying (AOB and NOB) and heterotrophic bacteria in the SBR:

$$OUR = \left(\frac{3.43 - Y_A}{Y_A}\right) \cdot \rho(1) + \left(\frac{1.14 - Y_N}{Y_N}\right) \cdot \rho(2) + \left(\frac{1 - Y_H}{Y_H}\right) \cdot \rho(3) \quad (2)$$

2.4. Design and validation of two methods for active biomass estimation

The estimation methods were based on the ASM1 model (modified as described in Eq. (1)). ASM1 provided the trajectory of the state variables throughout the cycle, including the concentrations of the initial and final AOB/NOB species. Two kinds of active biomass estimation method were designed: N-species Estimation (Nsp-E) and OUR Estimation (OUR-E). The first used off-line measurements of N-species concentrations as input for the estimation process; the second used on-line measurements such as DO, temperature and OUR profiles to calculate the internal variables of the nitrification process. The Nsp-E method uses ASM1 to convert the measurements of ammonium/nitrite/nitrate concentrations (mg L^{-1}) into OUR values (mg O_2 L^{-1}) and vice versa, which allowed us to validate the estimation of the OUR-E method online. Both methods require the initial concentrations of the N-species for each SBR cycle as input.

The estimation was carried out by running multiple simulations of the modified ASM1. At the beginning of the estimation process a vector with random concentrations of X_A, X_N and X_H was defined. With this vector the entire SBR cycle was simulated, generating an error of the estimation by comparison with the measured OUR profiles (for the OUR-E) or N-species (for the Nsp-E). A sequencing quadratic programming (SQP) algorithm, using quadratic approximation of the non-linear model, projected the trajectory of the estimation error by recursive changes of the initial vector. The estimation process ended when the estimated error converged to a minimum. This minimum was defined as a local minimum, so the estimation process was repeated with a large number of initial random vectors (Monte-Carlo Simulation). At the end of the simulation process the errors of all local minima were compared. The vector of the simulation with the smallest global error was set as the best fitting initial vector of the SBR cycles and used afterwards for the simulation of the trend of bacterial species X_A, X_N and X_H. This procedure was implemented in MATLAB® 7.1.

For running the model it was necessary to assign initial values for the bacteria concentrations (X_0) and an OUR profile resulting from the simulation (Outputs in Fig. 2). These are different for different X_0, which shows the observability of the applied X_0 (Ammar and Vivalda, 2004). Thus the model had different trajectories depending on the initial conditions used; the trajectory with the lowest error compared to measurements had to be found with a cost function.

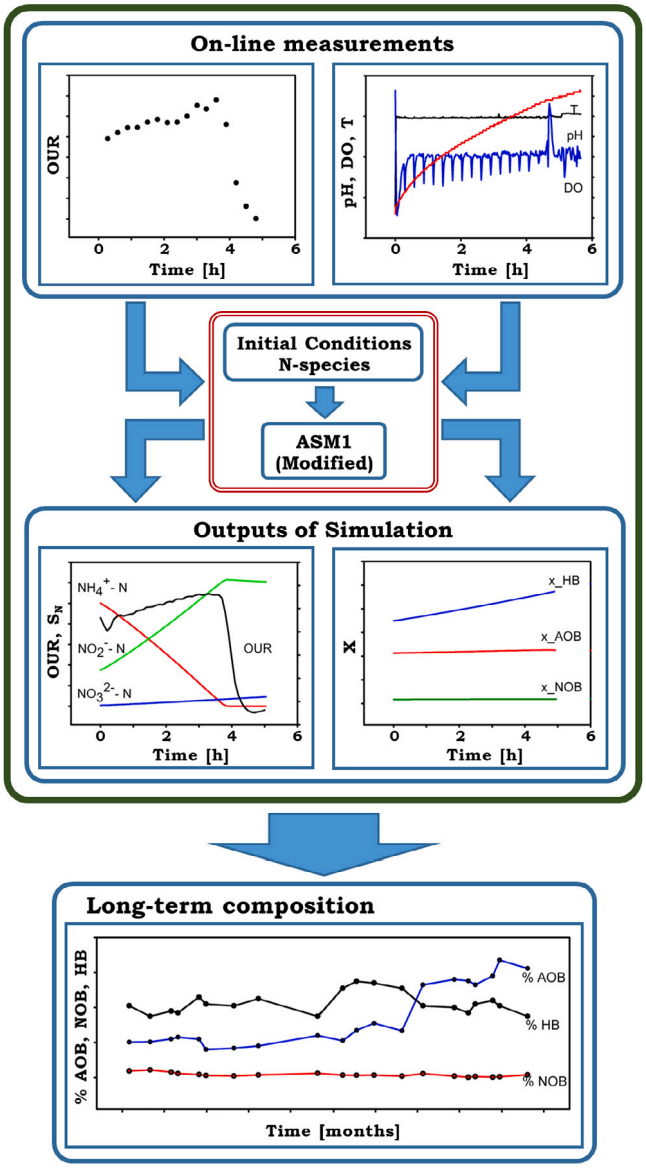

Fig. 2. Scheme of the active biomass estimation by OUR-E.

Nsp-E was mainly used for validation of OUR-E. Nsp-E measures more state variables than OUR-E, which demands a higher manual effort. However, Nsp-E is not measured online as it is with the OUR-E.

The two estimation methods were experimentally validated throughout a long-term SBR operation. The validation was performed over six months of SBR operation under unfavorable (120 days) and favorable conditions (60 days) for partial nitrification, according to the environment scenarios shown in Table 1.

The validation method was based on the examination for coherency of the results during long-term partial nitrification. On the one hand,

Table 2
Model matrix and kinetic equations of the ASM1 modified for partial nitrification.

	S_{TAN}	$S_{NO_2^-}$	$S_{NO_3^-}$	S_{ND}	S_S	X_A	X_N	X_H	X_P	X_S	X_{ND}	Rate equations
Aerobic growth of $\mathbf{X_A}$ (ρ(1))	$-\frac{1}{Y_A} - i_{XB}$	$\frac{1}{Y_A}$				1						$\mu_{max,A} \cdot \frac{S_{NH_3}}{K_{S,A} \cdot \left(1 + \frac{S_{HNO_2}}{K_{I,A}}\right) + S_{NH_3} + \left(\frac{S_{NH_3}^2}{K_{IS,A}}\right)} \cdot \left(\frac{S_{DO}}{K_{DO,A} + S_{DO}}\right) \cdot X_A$
Aerobic growth of $\mathbf{X_N}$ (ρ(2))	$-i_{XB}$	$-\frac{1}{Y_N} - i_{XB}$	$\frac{1}{Y_N}$				1					$\mu_{max,N} \cdot \frac{S_{HNO_2}}{K_{S,N} \cdot \left(1 + \frac{S_{NH_3}}{K_{I,N}}\right) + S_{HNO_2} + \left(\frac{S_{HNO_2}^2}{K_{IS,N}}\right)} \cdot \left(\frac{S_{DO}}{K_{DO,N} + S_{DO}}\right) \cdot X_N$
Aerobic growth of $\mathbf{X_H}$ (ρ(3))	$-i_{XB}$				$-\frac{1}{Y_H}$			1				$\mu_{max,H} \cdot \left(\frac{S_{DO}}{K_{O,H} + S_{DO}}\right) \cdot \left(\frac{S_S}{K_{S,H} + S_S}\right) \cdot X_H$
Decay of $\mathbf{X_A}$ (ρ(4))						−1			f_p	$1 - f_p$	$i_{XB} - f_p \cdot i_{XP}$	$b_A \cdot X_A$
Decay of $\mathbf{X_N}$ (ρ(5))							−1		f_p	$1 - f_p$	$i_{XB} - f_p \cdot i_{XP}$	$b_N \cdot X_N$
Decay of $\mathbf{X_H}$ (ρ(6))								−1	f_p	$1 - f_p$	$i_{XB} - f_p \cdot i_{XP}$	$b_H \cdot X_H$
Ammonification of $\mathbf{S_{ND}}$ (ρ(7))	1			−1								$k_a \cdot S_{ND} \cdot X_H$
Hydrolysis of $\mathbf{X_S}$ (ρ(8))					1					−1		$k_h \cdot \frac{X_S}{K_X + X_S/X_H} \cdot \frac{S_{DO}}{K_{O,H} + S_{DO}}$
Hydrolysis of $\mathbf{X_{ND}}$ (ρ(9))				1							−1	$k_h \cdot \frac{X_{ND}}{K_X + X_S/X_H} \cdot \frac{S_{DO}}{K_{O,H} + S_{DO}}$

Table 3
Stoichiometric and kinetic parameters for a two-step nitrification model (T, pH).
Source: Adapted from Jubany et al. (2008).

	Unit	Symbol	Value	Reference
Parameters related to AOB				
Oxygen saturation constant	mg O_2 L^{-1}	$K_{DO,A}$	0.99	Ciudad et al. (2007)
NH_3–N saturation constant	mg NH_3–N L^{-1}	$K_{S,A}$	0.3	Ciudad et al. (2007)
NH_3–N inhibition constant	mg NH_3–N L^{-1}	$K_{IS,A}$	540	Wiesmann (1994)
HNO_2–N inhibition constant	mg HNO_2–N L^{-1}	$K_{I,A}$	0.003	Jubany et al. (2008)
Growth yield	g COD g^{-1} N	Y_A	0.2	Wiesmann (1994)
Decay rate	h^{-1}	b_A	0.002	Wiesmann (1994)
Parameters related to NOB				
Oxygen saturation constant	mg O_2 L^{-1}	$K_{DO,N}$	1.4	Ciudad et al. (2007)
HNO_2–N saturation constant	mg HNO_2–N L^{-1}	$K_{S,N}$	2.2e−4	Ciudad et al. (2007)
HNO_2–N inhibition constant	mg HNO_2–N L^{-1}	$K_{IS,N}$	0.260	Wiesmann (1994)
NH_3–N inhibition constant	mg NH_3–N L^{-1}	$K_{I,N}$	0.010	Jubany et al. (2008)
Growth yield	g COD g^{-1} N	Y_N	0.06	Wiesmann (1994)
Decay rate	h^{-1}	b_N	0.002	Wiesmann (1994)
Parameters related to HB				
Affinity constant for S_{O_2}	mg O_2 L^{-1}	$K_{O,H}$	0.2	Henze et al. (2000)
Affinity constant for S_S	mg COD L^{-1}	K_S	4	Henze et al. (2000)
Growth yield	g COD g^{-1} COD	Y_H	0.67	Henze et al. (2000)
Decay rate	h^{-1}	b_H	0.008	Henze et al. (2000)
Other parameters				
Ammonification rate	L mg^{-1} COD h^{-1}	k_A	0.003	Henze et al. (2000)
Max. specific hydrolysis rate	g COD g^{-1} COD h^{-1}	K_H	0.13	Henze et al. (2000)
Affinity constant for X_S	g COD g^{-1} COD	K_x	0.03	Henze et al. (2000)
Nitrogen content of X_A, X_N, X_H	g N g^{-1} COD	i_{XB}	0.086	Henze et al. (2000)
Nitrogen content of X_P	g N g^{-1} COD	i_{XP}	0.06	Henze et al. (2000)
Fraction of biomass leading X_P	g COD g^{-1} COD	f_{XP}	0.08	Henze et al. (2000)

the concentration of AOB, NOB and HB obtained by both estimators (Nsp-E and OUR-E) must be in a reasonable range. On the other, the operating changes in the process from unfavorable to favorable conditions should be reflected by the long-term evolution of the bacterial concentrations.

The quality of the prediction of N-species concentrations and OUR values by OUR-E and Nsp-E, respectively, was evaluated using Theil's inequality coefficient (TIC) (Chen, 2011). Thus, the goodness of fit of each estimation method was quantified by comparing the simulation

Table 4
Kinetic parameters and equilibrium equations for nitritation and nitratation.

Name	Unit	Equation	Reference
Ionization constant for ammonium	–	$K_a = e^{(6334/(273+T))}$	Jubany et al. (2008)
Ionization constant for nitrous acid	–	$K_n = e^{(-2300/(273+T))}$	Jubany et al. (2008)
Maximum specific growth rate (AOB)	h^{-1}	$\mu_{max,A} = \frac{1.28 \times 10^{12} \cdot e^{(-8183/(273+T))}}{1 + \left(\frac{2.05 \times 10^{-9}}{10^{-pH}}\right) + \left(\frac{10^{-pH}}{1.66 \times 10^{-7}}\right)} \cdot \frac{1}{24}$	Jubany et al. (2008)
Maximum specific growth rate (NOB)	h^{-1}	$\mu_{max,N} = \frac{6.69 \times 10^{7} \cdot e^{(-5295/(273+T))}}{1 + \left(\frac{2.05 \times 10^{-9}}{10^{-pH}}\right) + \left(\frac{10^{-pH}}{1.66 \times 10^{-7}}\right)} \cdot \frac{1}{24}$	Jubany et al. (2008)
Maximum specific growth rate (HB)	h^{-1}	$\mu_{max,H} = 6 \cdot (1.07)^{(T-20)} \cdot \frac{1}{24}$	Jubany et al. (2008)
Concentration of NH_3–N	$\frac{mg\ N}{L}$	$S_{NH_3} = \frac{S_{TAN} \cdot 10^{pH}}{K_a + 10^{pH}}$	Jubany et al. (2008)
Concentration of HNO_2–N	$\frac{mg\ N}{L}$	$S_{HNO_2} = \frac{S_{NO_2^-}}{1 + K_n \cdot 10^{pH}}$	Jubany et al. (2008)

Table 5
Comparison of average experimental parameters of favorable and unfavorable stages with estimations and references.

Reference	Process conditions				Experimental data				Biomass fraction estimation
	pH	SRT	T	DO	r_s	β	OUR	VSS	$X_N/(X_A + X_N)$
		[d]	[°C]	[mg/L]	[kg TAN/(kg VSS·d)]	[%]	[mg O_2/(L·h)]	[mg/L]	[%]
Unfavorable scenario	7.6	40	16–23	2.0	0.38 ± 0.16	48.5 ± 15.7	80.2 ± 10.7	4935 ± 930	11.8 ± 3.7 (Nsp-E) 10.3 ± 6.6 (OUR-E)
Favorable scenario	8.5	10	16–23	2.0	0.77 ± 0.11	79.6 ± 6.7	77.2 ± 15.7	3095 ± 287	3.1 ± 1.0 (Nsp-E) 1.6 ± 1.4 (OUR-E)
Pollice et al. (2002)	> 7.2	40	32	2.0	0.11	–	–	–	–
Pollice et al. (2002)	> 7.2	10	32	2.0	0.62	–	–	–	–
Jianlong and Ning (2004)	7.5	–	30	1.5	2.76	–	–	–	–
Jianlong and Ning (2004)	8.5	–	30	1.5	2.21	–	–	–	–
Jubany et al. (2009)	8.3	30	25 ± 1	1.4 ± 0.2	0.4 ± 0.1	100	~ 68	–	< 1
Rongsayamanont et al. (2010)	7.5–8.2	–	22–23	4.5–7.5	–	0	–	–	10.3 ± 3.7 (Nsp-E) 4.4 ± 4 (OUR-E)
Guo et al. (2009)	7.0–7.8	30	18–25 12–17	0–4	0.06	> 90	–	–	0.5–3.5

and measurements variables as follows:

$$TIC_{Sp,n} = \frac{\sqrt{\sum_i y_i - \hat{y}_{m,i}}}{\sqrt{\sum_i y_i^2} + \sqrt{\sum_i \hat{y}_{m,i}^2}} \quad (3)$$

$$TIC_{Tot} = \sum_1^n TIC_{Sp,n} \quad (4)$$

$$TIC_{OUR} = \frac{\sqrt{\sum_i OUR_i - \hat{OUR}_{m,i}}}{\sqrt{\sum_i OUR_i^2} + \sqrt{\sum_i \hat{OUR}_{m,i}^2}} \quad (5)$$

The coincidence of measurements and simulation of every nitrogen species was determined by Eq. (3). For a total TIC of the N-species, Eq. (4) was applied. Eq. (5) shows the calculation of the TIC of OUR simulations and measurements, where $y_{m,i}$ and $OUR_{m,i}$ are the measurements, and $\hat{y}_{m,i}$ and $\hat{OUR}_{m,i}$ are the estimates made at the same time as the measurements with the optimal initial conditions of the calculated state vector by both estimation methods. The TIC has a value between 0 and 1. Good model adaptation to the measurements is indicated by a TIC smaller than 0.3 (Huiliñir et al., 2010).

3. Results and discussion

3.1. Partial nitrification in a real-time controlled SBR

SBR operation was modeled based on a modified ASM1 to describe the two-step nitrification process: nitritation and nitratation. Fig. 3 shows two different cycles, named cycle 4 (on the left side) and cycle 7 (on the right side); both cycles were operated at pH = 7.6 and SRT = 40 d.

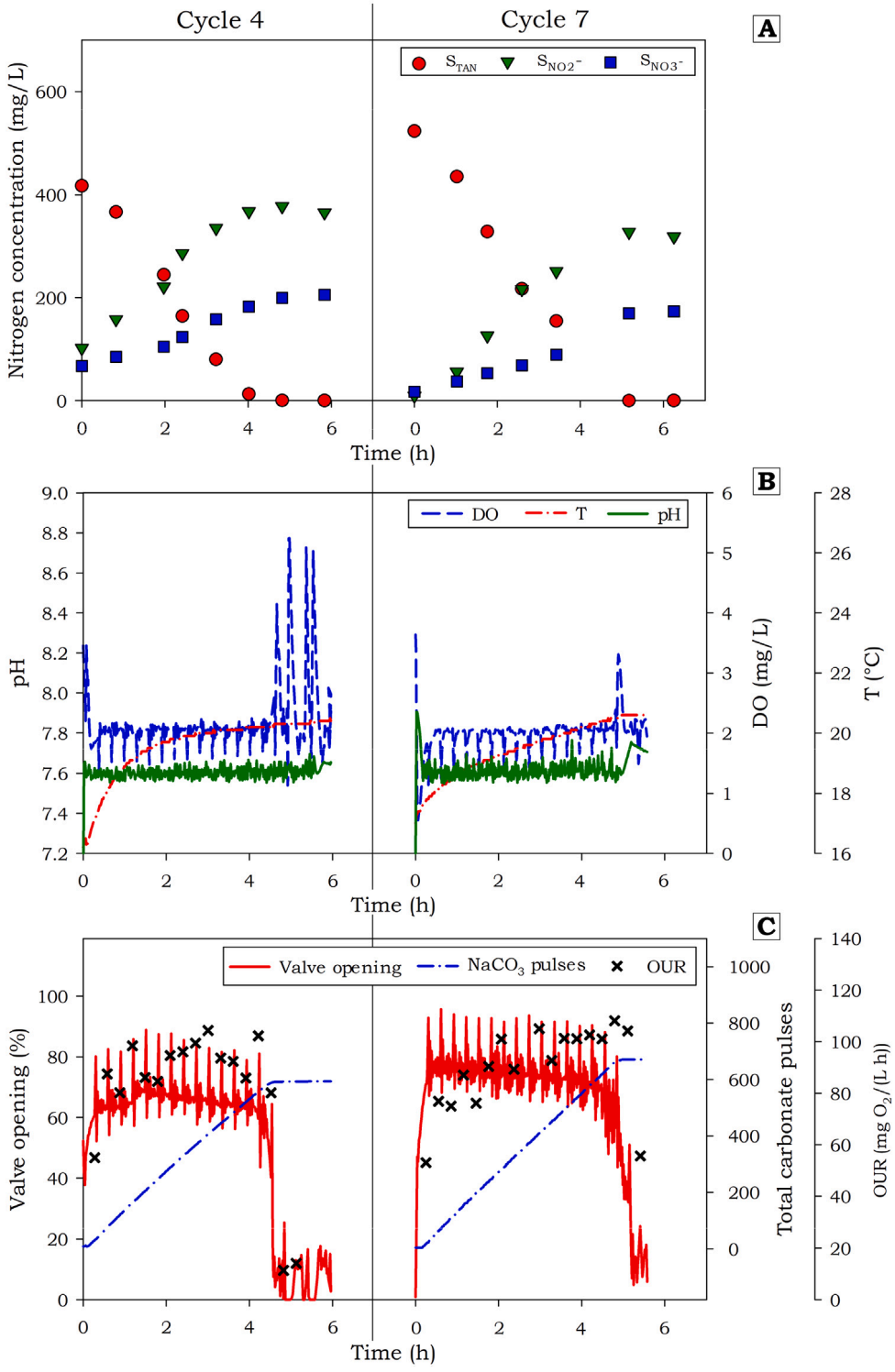

Fig. 3. Partial nitrification for two SBR cycles conducted under unfavorable conditions, pH = 7.6 and SRT = 40 d. (A) Concentrations of nitrogen species; (B) on-line temperature T, DO concentration and pH value; (C) manipulated variables of pH and DO control systems: Valve opening (%)-Carbonate pulses, and on-line OUR measurement.

Fig. 3A shows the evolution of the nitrogen species during partial nitrification. The ammonia oxidation rate was close to 0.27 kg TAN/(kg VSS·d) with an ammonia conversion of over 99% in both cycles. The initial concentrations of TAN were over 400 mg N/L (> 6 mg NH_3-N/L) for both cycles, enabling ammonia cross inhibition on the NOB ($K_{I,N}$ = 0.01 mg NH_3-N/L). Fig. 3 shows a significant level of inhibition of nitratation in cycles 4 and 7, which led to a nitrite accumulation of over 66% in those assays.

Fig. 3B shows the evolution of temperature and the real-time controlled curves of pH and DO concentration during cycles 4 and 7. The predictive control set the DO concentration around 2 mg/L; the air supply was interrupted every fifteen minutes for measurement of the OUR. The DO concentration and the pH (set-point 7.6), were controlled by means of the manipulated variables air valve (%) opening and Na_2CO_3 pulses, as shown in Fig. 3C. The alkaline solution was added

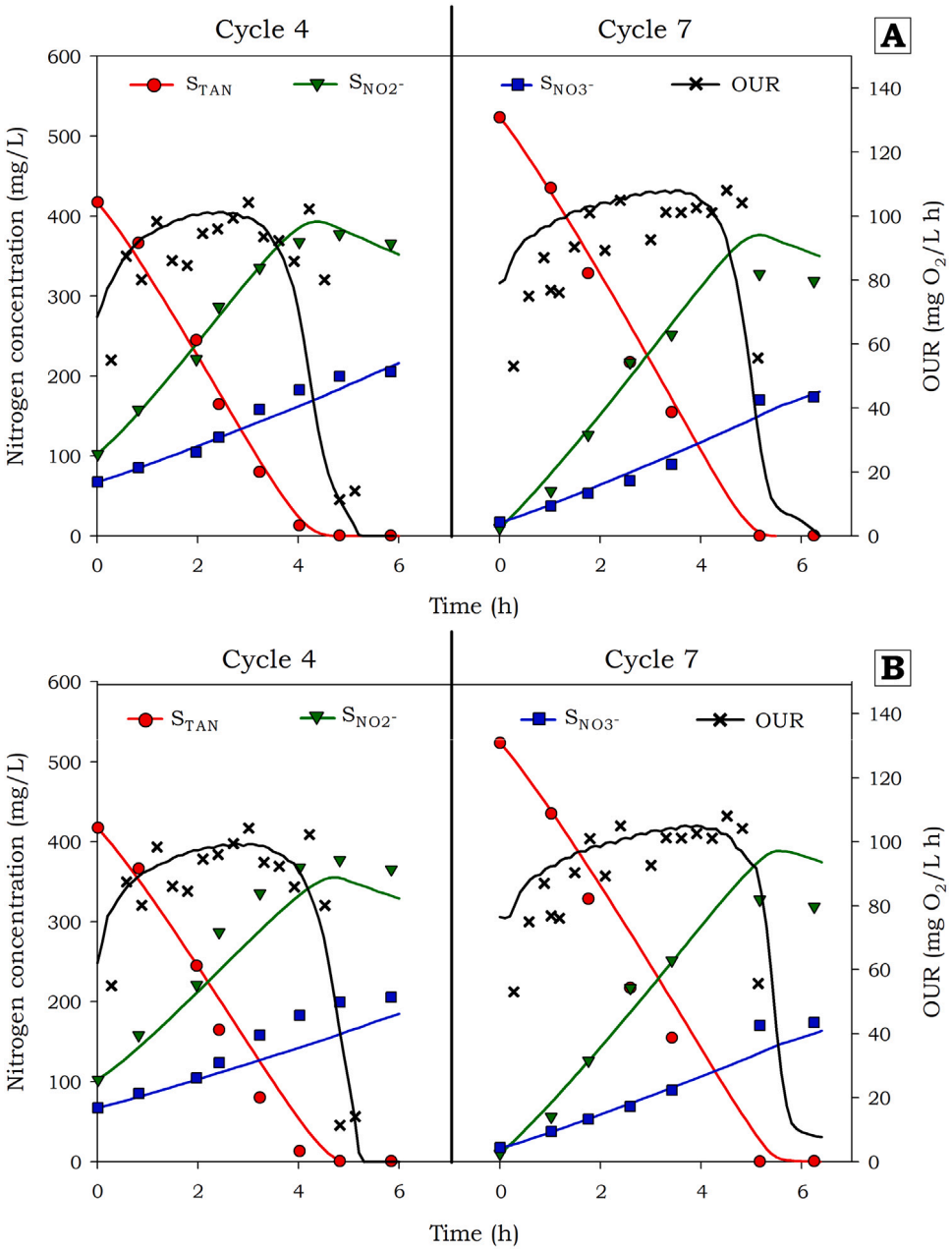

Fig. 4. Performance of Nsp-E and OUR-E under unfavorable conditions for partial nitrification, pH = 7.6 and SRT = 40 d. (A) Nsp-E: Modeling of nitrogen species concentrations and prediction of OUR (B) OUR-E: Modeling of OUR and prediction of nitrogen species concentrations.

step-wise to neutralize acidification during ammonia oxidation, achieving a plateau around 600 pulses at the end-point of nitrification. Air valve opening increased at the beginning to maintain the DO set-point and decreased after four hours when the ammonia was completely oxidized. The DO concentration and the pH values rose at the endpoint of ammonia oxidation.

Fig. 3C illustrates bending points in profiles of all secondary variables: %AVO, number of sodium carbonate pulses, and ORP. The bending points for cycles 4 and 7 occurred at 4.5 and 5 h, respectively, at the end of TAN oxidation. The mean value of the %AVO sank slowly during the reaction, until it plunged almost instantaneously to values below 20% in cycle 4 (%AVO bending point). Fig. 3C shows in both cycles that the total number of sodium pulses increased in a nearly linear mode until the constant number of total pulses reached marked the end of TAN oxidation (carbonate consumption bending point). The OUR values increased during both cycles, indicating a higher respiration rate, until falling instantaneously below 60 mg/(L·h) at the end of TAN oxidation (OUR Bending Point). These three ways of determining the end-point of nitrification were observable during all the cycles performed.

3.2. Design of Nsp-E and OUR-E estimators

This section presents the internal variables of the nitrification process calculated by the Nsp-E and OUR-E estimators for two scenarios. The first scenario shows cycles 4 and 7 operating under unfavorable conditions, and the second shows cycles 18 and 23 operating under favorable conditions for partial nitrification.

3.2.1. Estimation under unfavorable conditions: pH = 7.6 and SRT 40 d

Fig. 4 shows the curves of N-species and OUR estimated by Nsp-E (Fig. 4A) and OUR-E (Fig. 4B) under unfavorable conditions. As

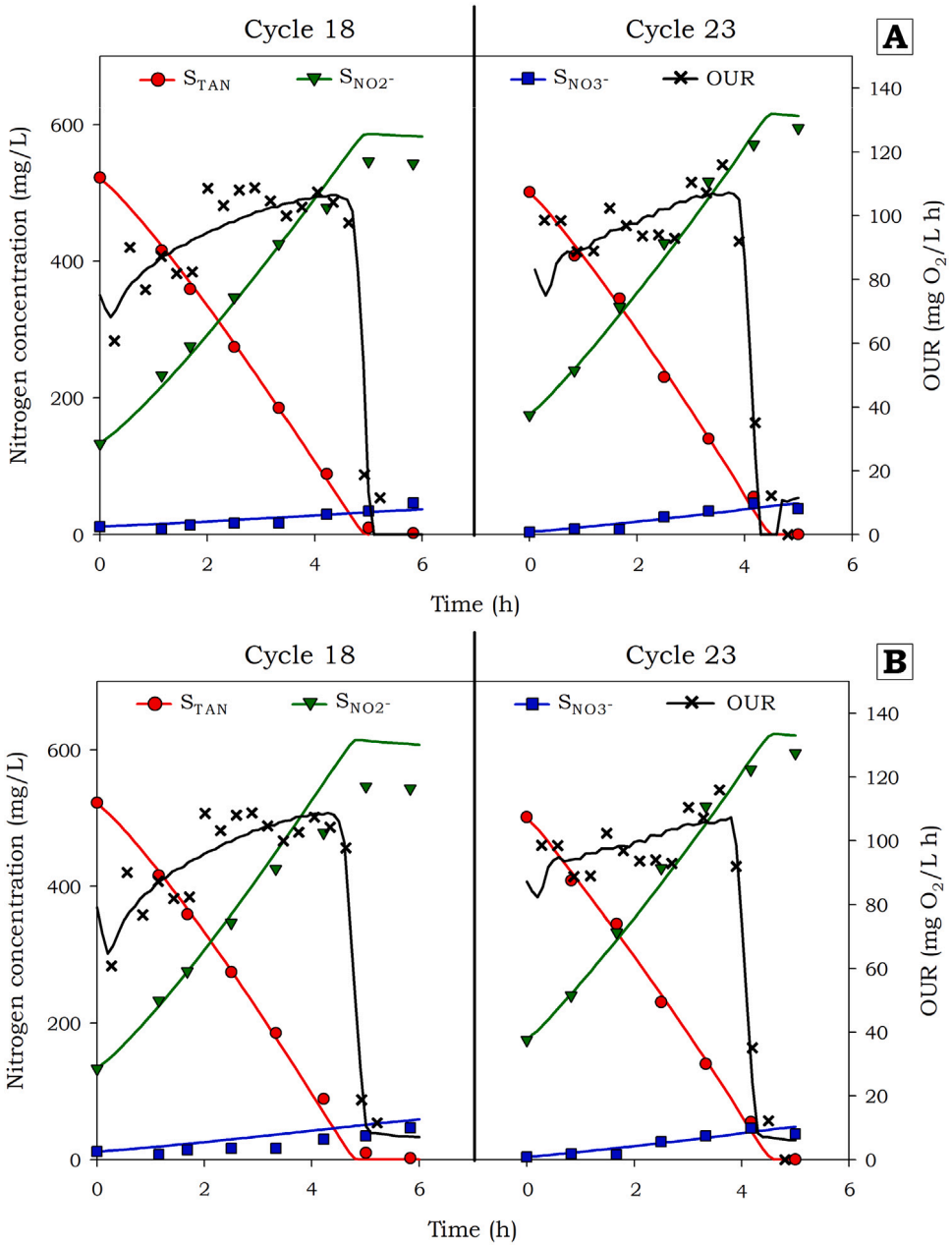

Fig. 5. Performance of Nsp-E and OUR-E under favorable conditions for partial nitrification, pH = 8.5 and SRT = 10 d. (A) Nsp-E: Modeling of nitrogen species concentrations and prediction of OUR (B) OUR-E: Modeling of OUR and prediction of nitrogen species concentrations.

illustrated in Fig. 4A, the Nsp-E estimation shows a high coincidence among the measured and simulated curves of N-species concentrations for cycles 4 and 7; the algorithm slightly overestimates the concentration of nitrite at the end of cycle 7. The TIC_{tot} value was 0.034, indicating very good agreement with measured data (TIC < 0.3). It is noteworthy that Nsp-E was able to estimate adequately the OUR experimental values, with TIC values ranging from 0.069 to 0.076, although the Nsp-E used off-line measurements of N-species for the estimation process. Fig. 4B shows the performance of OUR-E. The simulated OUR curve resulted in a closer agreement with the experimental values than the OUR prediction of the Nsp-E (Fig. 4A); however, the figure shows a minor overestimation in cycle 7. Based on these data the TIC_{OUR} were calculated to be 0.026 and 0.005 for cycles 7 and 4, respectively. The initial conditions obtained with OUR-E were used to predict the N-species curves. As can be seen in Fig. 4B, the agreement with experimental N-species was good, achieving a TIC_{Tot} of 0.065 for both cycles.

In all 17 cycles (120 operation days) performed by Nsp-E the average TIC were calculated to be TIC_{tot} = 0.04 and TIC_{OUR} = 0.36. For the OUR-E, the average TIC were calculated to be TIC_{tot} = 0.12 and TIC_{OUR} = 0.02. Based on the experimental results, the OUR-E has a better quality of prediction than the Nsp-E, which can be explained by the experimental data size of the OUR used as input during the estimation process.

3.3. Estimation under favorable conditions: pH = 8.5 and SRT 10 d

Fig. 5 shows the curves of N-species and OUR estimated by Nsp-E (Fig. 5A) and OUR-E (Fig. 5B) under favorable conditions. As shown in Fig. 5A the Nsp-E estimation shows a high coincidence between the measured and calculated data for cycles 18 and 23. The TIC_{tot} value was lower than 0.053 indicating a very good agreement (TIC < 0.3) with measured data for nitrogen species concentrations. Nsp-E was also able

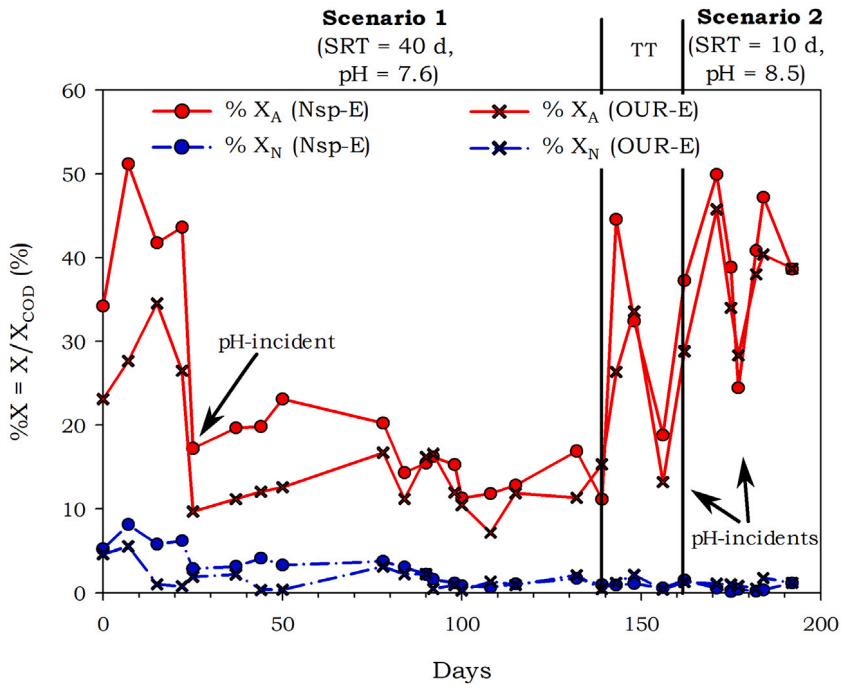

Fig. 6. Bacterial active fractions of AOB (X_A) and NOB (X_N) calculated by Nsp-E and OUR-E in a long term SBR operation. Total COD particulate $X_{COD} = X_A + X_N + X_H + X_P + X_S$.

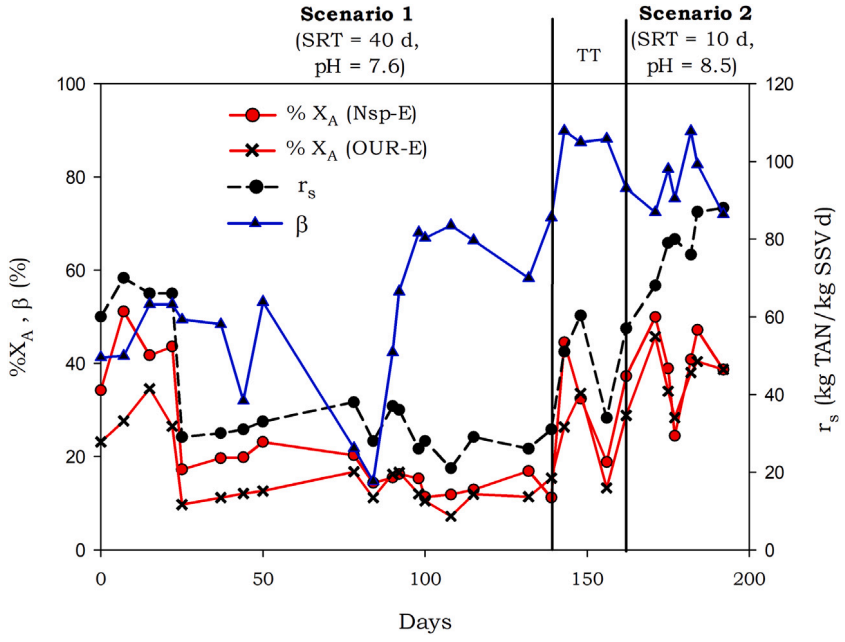

Fig. 7. Evolution of the active AOB fraction and the experimental total ammonia nitrogen oxidation rate (r_s) in a long term SBR operation.

to estimate adequately the OUR experimental values, with TIC values ranging from 0.022 (cycle 23) to 0.083 (cycle 18).

Fig. 5B shows that the simulated OUR curve of the OUR-E resulted in a better coincidence with the experimental values than the OUR prediction of the Nsp-E (Fig. 5A). Based on these data, the TIC_{OUR} were calculated to be 0.018 and 0.011 for cycles 18 and 23 respectively. The initial conditions obtained with OUR-E were used to predict the N-species concentrations. As can be seen in Fig. 5B, the agreement with N-species measurements was good, achieving a TIC_{Tot} ranging from 0.046 (cycle 18) to 0.086 (cycle 23). Contrary to the unfavorable scenario, under the favorable operating condition for partial nitrification the bending points in the OUR curves agreed with experimental measurements at the end of ammonia oxidation. The latter could be explained by an improvement in the experimental measurements of OUR in time, which led to better prediction of the N-species during the favorable scenario than the unfavorable scenario. Thus the TIC values of TAN and nitrite diminished by 11% and 68% when the SBR was shifted to the favorable condition.

For the whole 22 SBR cycles operated under favorable and unfavorable conditions for partial nitrification, the estimation of the N-species concentrations by OUR-E was significantly better (TIC = 0.124 ± 0.01) than the estimation of the OUR by Nsp-E (TIC = 0.316 ± 0.06). The OUR-E was able to predict correctly (TIC < 0.3) the concentrations of ammonia, nitrite and nitrate using only one experimental source

of kinetic information: OUR measurements every 15 min. The higher information density of the on-line OUR measurements used as input by the OUR-E, with fewer manual errors than in the off-line measurements of nitrogen species used by Nsp-E, explains the better performance of the OUR-E.

3.4. Validation of OUR estimator on long-term SBR operation

The OUR-E aimed to monitor the dynamic behavior of nitrifying active biomass on a long-term basis under different SBR operating scenarios. Fig. 6 shows the active nitrifying bacteria estimation using Nsp-E and OUR-E during SBR operation for more than 6 months. During scenario 1 (unfavorable for partial nitrification), the fraction of active AOB (X_A) with respect to the total particulate COD concentration diminished to approximately 15% after three months' operation. As shown in Fig. 6, after 50 days Nsp-E and OUR-E estimated similar active biomass fractions. After 30 d of operation at scenario 2 (favorable for partial nitrification) the AOB fraction increased by up to 40% and the NOB fraction diminished to 1%–3%. A reduction of SRT by a factor of 4 (40 to 10 d) in scenario 2 promoted a kinetic of selective NOB washout. On the other hand, at pH = 8.5 the ammonia concentration appeared as the real substrate for AOB and an inhibition factor for NOB, enhancing the AOB/NOB ratio. Regarding the total bacteria concentration, Jubany et al. (2009) reported fractions of X_A = 68%, X_N < 1% and X_H = 31% based on fluorescent in-situ hybridization (FISH) analysis for partial nitrification with 100% nitrite accumulation during 100 d operation of a continuous reactor system. In this work, the OUR-E estimated active biomass fractions of X_A = 39.8%, X_N = 1.3% and X_H = 58.9% as mean values for partial nitrification with 86% nitrite accumulation during 60 d of SBR operation (scenario 2 plus transition period). Fig. 6 also shows the effect of two pH incidents on the nitrifying biomass, which have a noticeable effect on the Nsp-E and OUR-E trends.

Fig. 7 shows the evolution of the AOB active biomass fraction as a function of the ammonia conversion rate (r_s) and nitrite accumulation (β). The AOB estimations of both Nsp-E and OUR-E follow the dynamic of the ammonia oxidation rate (experimental measurements) in long-term SBR operation. At the end of scenario 1, the nitrite accumulation started to rise according to the decay of the NOB fraction. During scenario 2 the nitrite accumulation increased up to 90% owing to the simultaneous increase of the AOB and decay of NOB (see Fig. 6).

Table 5 compares the different results of this work with the literature. Despite unfavorable conditions for partial nitrification at SRT = 40 d and pH = 7.6, the nitrite accumulation remained close to 50%. Hence, a low DO concentration around 2 mg/L was enough to limit NOB growth during more than 100 days of operation under unfavorable conditions. The favorable scenario at SRT = 10 d and pH = 8.5 almost doubled nitrite accumulation, which put the accent on the role of free ammonia nitrogen for reaching stable partial nitrification on a long-term basis. The TAN oxidation rate increased strongly from 0.38 to 0.77 when the pH was increased by one point (SRT = 10 d does not limit AOB growth), emphasizing the importance of putting the reactor out of limitation by ammonia for AOB growth. In terms of the volumetric reaction rate, the TAN oxidation rate increased from 1.38 ± 0.3 to 1.71 ± 0.03 kg TAN/(m^3·d). The TAN oxidation values were in the order of magnitude reported in the literature (Pollice et al., 2002; Ciudad et al., 2005; Jubany et al., 2009).

As shown in Table 5, the OUR values did not change significantly from one scenario to another, hence OUR would not work as a control variable, at least to conduct partial nitrification from 50% to over 80% of nitrite accumulation. The latter results move away from the OUR strategy reported in Jubany et al. (2009). Remarkably, the OUR-E was able to predict a significant reduction in the NOB active fraction from 10.3% to 1.6% of the autotrophic biomass when the scenario shifted to a favorable condition for partial nitrification. This estimation of the NOB fraction in a favorable scenario agrees with those reported by Guo et al. (2009).

We concluded that the OUR-E is able to adequately estimate the nitrifying active biomass during a process of partial nitrification using OUR on-line measurements as experimental data source. This work validated the OUR-E with 200 days by comparing it with the Nsp-E; both estimation methods predicted similar nitrifying active biomass during two operating scenarios on a long-term basis.

4. Conclusions

Two methods for active bacteria estimation were designed and validated using on-line OUR measurements every 15 min (OUR-E) and off-line measurements of nitrogen species (Nsp-E) as input data for process estimation. Both estimation methods predicted similar active nitrifying and heterotrophic biomass concentrations during the two operating scenarios. The estimation of the N-species concentrations by OUR-E was significantly better (TIC = 0.124 ± 0.01) than the estimation of the OUR values by Nsp-E (mean TIC = 0.316 ± 0.06) according to the Theil's coefficient of inequality. The OUR-E was able to predict a significant reduction in the NOB active fraction from 10.3% to 1.6% when the scene shifted to a favorable condition for partial nitrification. The opposite trend of NOB occurred during consecutive SBR cycles (200 days). We concluded that the OUR-E could adequately estimate the nitrifying active biomass concentration during a process of partial nitrification using OUR on-line measurements as a sole experimental source for long-term SBR operations. The main contribution of the paper was to use phenomenological knowledge given by the ASM1 to estimate the dynamics of active bacteria concentrations in an SBR, as well as, in consecutive batch-cycles. This knowledge will allow us to make effective selective pressure strategies to keep NOB growth under permanent inhibition/limitation conditions in the reactor while achieving stable partial nitrification on a long-term basis.

CRediT authorship contribution statement

Franklin Lindow: Software, Investigation, Writing - original draft. **Carlos Muñoz:** Formal analysis, Supervision, Writing - review & editing. **Francisco Jaramillo:** Methodology, Writing - review & editing. **Robert H. Bishop:** Writing - review & editing. **José B. Proal-Nájera:** Conceptualization. **Christian Antileo:** Writing - original draft, Writing - review & editing, Supervision, Project administration.

Declaration of competing interest

The authors declare that they have no known competing financial interests or personal relationships that could have appeared to influence the work reported in this paper.

Acknowledgments

The work of Francisco Jaramillo was supported by a Ph.D scholarship from ANID, Chile. ANID-PCHA/Doctorado Nacional (grant number 2014-21140201).

References

Alcaraz-González, V., Harmand, J., Rapaport, A., Steyer, J.P., González-Alvarez, V., Pelayo-Ortiz, C., 2002. Software sensors for highly uncertain WWTPs: a new approach based on interval observers. Water Res. 36 (10), 2515–2524. http://dx.doi.org/10.1016/S0043-1354(01)00466-3.

Ammar, S., Vivalda, J.C., 2004. On the preservation of observability under sampling. Systems Control Lett. 52 (1), 7–15. http://dx.doi.org/10.1016/j.sysconle.2003.08.008.

Antileo, C., Medina, H., Bornhardt, C., Muñoz, C., Jaramillo, F., Proal, J., 2013. Actuators monitoring system for real-time control of nitrification—denitrification via nitrite on long term operation. Chem. Eng. J. 223, 467–478. http://dx.doi.org/10.1016/j.cej.2013.02.079.

Benazzi, F., Gernaey, K.V., Jeppsson, U., Katebi, R., 2007. On-line estimation and detection of abnormal substrate concentrations in WWTPs using a software sensor: a benchmark study. Environ. Technol. 28 (8), 871–882. http://dx.doi.org/10.1080/09593332808618852.

Boaventura, K.M., Roqueiro, N., Coelho, M.A.Z., Araújo, O.Q.F., 2001. State observers for a biological wastewater nitrogen removal process in a sequential batch reactor. Bioresour. Technol. 79 (1), 1–14. http://dx.doi.org/10.1016/S0960-8524(01)00041-4.

Bogaerts, P., Wouwer, A.V., 2003. Software sensors for bioprocesses. ISA Trans. 42 (4), 547–558. http://dx.doi.org/10.1016/S0019-0578(07)60005-6.

Boulkroune, B., Darouach, M., Zasadzinski, M., Gillé, S., Fiorelli, D., 2009. A nonlinear observer design for an activated sludge wastewater treatment process. J. Process Control. 19 (9), 1558–1565. http://dx.doi.org/10.1016/j.jprocont.2009.07.017.

Casellas, M., Dagot, C., Baudu, M., 2006. Set up and assessment of a control strategy in a SBR in order to enhance nitrogen and phosphorus removal. Process Biochem. 41 (9), 1994–2001. http://dx.doi.org/10.1016/j.procbio.2006.04.012.

Chen, J., 2011. Comparison analysis for validating methods of system simulation models. In: 2011 International Conference on Electric Information and Control Engineering. pp. 232–235. http://dx.doi.org/10.1109/ICEICE.2011.5778078.

Chen, W.B., Tian, M., Wang, R.R., Liu, F., 2012. Application of pH, DO and OUR control for short-cut nitrification. In: Renewable and Sustainable Energy, Advanced Materials Research. Trans Tech Publications Ltd, pp. 2112–2116. http://dx.doi.org/10.4028/www.scientific.net/AMR.347-353.2112.

Ciudad, G., González, R., Bornhardt, C., Antileo, C., 2007. Modes of operation and pH control as enhancement factors for partial nitrification with oxygen transport limitation. Water Res. 41 (20), 4621–4629. http://dx.doi.org/10.1016/j.watres.2007.06.036.

Ciudad, G., Rubilar, O., Muñoz, P., Ruiz, G., Chamy, R., Vergara, C., Jeison, D., 2005. Partial nitrification of high ammonia concentration wastewater as a part of a shortcut biological nitrogen removal process. Process Biochem. 40 (5), 1715–1719. http://dx.doi.org/10.1016/j.procbio.2004.06.058.

Corominas, L., Sin, G., Puig, S., Balaguer, M.D., Vanrolleghem, P.A., Colprim, J., 2011. Modified calibration protocol evaluated in a model-based testing of SBR flexibility. Bioprocess Biosyst. Eng. 34 (2), 205–214. http://dx.doi.org/10.1007/s00449-010-0462-2.

Ganesh, R., Balaji, G., Ramanujam, R.A., 2006. Biodegradation of tannery wastewater using sequencing batch reactor - respirometric assessment. Bioresour. Technol. 97 (15), 1815–1821. http://dx.doi.org/10.1016/j.biortech.2005.09.003.

Garcia-Ochoa, F., Gomez, E., Santos, V.E., Merchuk, J.C., 2010. Oxygen uptake rate in microbial processes: An overview. Biochem. Eng. J. 49 (3), 289–307. http://dx.doi.org/10.1016/j.bej.2010.01.011.

Gernaey, K.V., van Loosdrecht, M.C.M., Henze, M., Lind, M., Jorgensen, S.B., 2004. Activated sludge wastewater treatment plant modelling and simulation: state of the art. Environ. Model. Softw. 19 (9), 763–783. http://dx.doi.org/10.1016/j.envsoft.2003.03.005.

Guo, J., Peng, Y., Wang, S., Zheng, Y., Huang, H., Ge, S., 2009. Effective and robust partial nitrification to nitrite by real-time aeration duration control in an SBR treating domestic wastewater. Process Biochem. 44 (9), 979–985. http://dx.doi.org/10.1016/j.procbio.2009.04.022.

Hedegärd, M., Wik, T., 2011. An online method for estimation of degradable substrate and biomass in an aerated activated sludge process. Water Res. 45 (19), 6308–6320. http://dx.doi.org/10.1016/j.watres.2011.09.003.

Henze, M., Grady, Jr., C.P.L., Gujer, W., Marais, G.V.R., Matsuo, T., 1987. Activated Sludge Model No. 1. IAWPRC Scientific and Technical Report No. 1, IAWPRC, London.

Henze, M., Gujer, W., Mino, T., Van Loosdrecht, M., 2000. Activated Sludge Models ASM1, ASM2, ASM2d and ASM3. IWA Scientific and Technical Report, IWA Publishing, p. 128. http://dx.doi.org/10.2166/9781780402369.

Hockenbury, M.R., Grady, C.P.L., 1977. Inhibition of nitrification-effects of selected organic compounds. J. (Water Pollut. Control Fed.). 49 (5), 768–777.

Huiliñir, C., Romero, R., Muñoz, C., Bornhardt, C., Roeckel, M., Antileo, C., 2010. Dynamic modeling of partial nitrification in a rotating disk biofilm reactor: Calibration, validation and simulation. Biochem. Eng. J. 52 (1), 7–18. http://dx.doi.org/10.1016/j.bej.2010.06.012.

Jaramillo, F., Orchard, M., Muñoz, C., Antileo, C., Sáez, D., Espinoza, P., 2018a. On-line estimation of the aerobic phase length for partial nitrification processes in SBR based on features extraction and SVM classification. Chem. Eng. J. 331 (suppl. C), 114–123. http://dx.doi.org/10.1016/j.cej.2017.07.185.

Jaramillo, F., Orchard, M., Muñoz, C., Zamorano, M., Antileo, C., 2018b. Advanced strategies to improve nitrification process in sequencing batch reactors - A review. J. Environ. Manag. 218, 154–164. http://dx.doi.org/10.1016/j.jenvman.2018.04.019.

Jianlong, W., Ning, Y., 2004. Partial nitrification under limited dissolved oxygen conditions. Process Biochem. 39 (10), 1223–1229. http://dx.doi.org/10.1016/S0032-9592(03)00249-8.

Jubany, I., Carrera, J., Lafuente, J., Baeza, J.A., 2008. Start-up of a nitrification system with automatic control to treat highly concentrated ammonium wastewater: Experimental results and modeling. Chem. Eng. J. 144 (3), 407–419. http://dx.doi.org/10.1016/j.cej.2008.02.010.

Jubany, I., Lafuente, J., Baeza, J.A., Carrera, J., 2009. Total and stable washout of nitrite oxidizing bacteria from a nitrifying continuous activated sludge system using automatic control based on Oxygen Uptake Rate measurements. Water Res. 43 (11), 2761–2772. http://dx.doi.org/10.1016/j.watres.2009.03.022.

Muñoz, C., Young, H., Antileo, C., Bornhardt, C., 2009. Sliding mode control of dissolved oxygen in an integrated nitrogen removal process in a sequencing batch reactor (SBR). Water Sci. Technol. 60 (10), 2545–2553. http://dx.doi.org/10.2166/wst.2009.516.

Pambrun, V., Paul, E., Spérandio, M., 2008. Control and modelling of partial nitrification of effluents with high ammonia concentrations in sequencing batch reactor. Chem. Eng. Process. Process Intensif. 47 (3), 323–329. http://dx.doi.org/10.1016/j.cep.2007.01.028.

Peng, Y., Zhu, G., 2006. Biological nitrogen removal with nitrification and denitrification via nitrite pathway. Appl. Microbiol. Biotechnol. 73 (1), 15–26. http://dx.doi.org/10.1007/s00253-006-0534-z.

Pollice, A., Tandoi, V., Lestingi, C., 2002. Influence of aeration and sludge retention time on ammonium oxidation to nitrite and nitrate. Water Res. 36 (10), 2541–2546. http://dx.doi.org/10.1016/S0043-1354(01)00468-7.

Rongsayamanont, C., Limpiyakorn, T., Law, B., Khan, E., 2010. Relationship between respirometric activity and community of entrapped nitrifying bacteria: Implications for partial nitrification. Enzyme Microb. Technol. 46 (3), 229–236. http://dx.doi.org/10.1016/j.enzmictec.2009.10.014.

Smida, F., Ladhari, T., Hadj Saïd, S., M'Sahli, F., 2018a. Unknown inputs nonlinear observer for an activated sludge process. Math. Probl. Eng. 2018, http://dx.doi.org/10.1155/2018/1382914.

Smida, F., Ladhari, T., Hadj Saïd, S., M'Sahli, F., 2018b. Unknown inputs observer-based output feedback predictive controller for an activated sludge process. IETE J. Res. (July), http://dx.doi.org/10.1080/03772063.2018.1497553.

Sotomayor, O.A.Z., Park, S.W., Garcia, C., 2002. Software sensor for on-line estimation of the microbial activity in activated sludge systems. ISA Trans. 41 (2), 127–143. http://dx.doi.org/10.1016/S0019-0578(07)60073-1.

Turk, O., Mavinic, D.S., 1989. Maintaining nitrite build-up in a system acclimated to free ammonia. Water Res. 23 (11), 1383–1388. http://dx.doi.org/10.1016/0043-1354(89)90077-8.

Wiesmann, U., 1994. Biological nitrogen removal from wastewater. In: Biotechnics/Wastewater SE - 5, Advances in Biochemical Engineering/Biotechnology. Springer Berlin Heidelberg, pp. 113–154. http://dx.doi.org/10.1007/BFb0008736.

Wu, J., Yan, G., Zhou, G., Xu, T., 2014. Model predictive control of biological nitrogen removal via partial nitrification at low carbon/nitrogen (C/N) ratio. J. Environ. Chem. 2 (4), 1899–1906. http://dx.doi.org/10.1016/j.jece.2014.08.007.